Journal of Organometallic Chemistry 880 (2019) 187–195

Contents lists available at ScienceDirect

Journal of Organometallic Chemistry

journal homepage: www.elsevier.com/locate/jorganchem

La-mediated dehydrogenation and C–C bond cleavage of 1,4-pentadiene and 1-pentyne: Spectroscopy and formation of La(C_5H_6) and La(C_3H_4) radicals

Wenjin Cao, Yuchen Zhang, Dong-Sheng Yang*

Department of Chemistry, University of Kentucky, Lexington, KY, 40506-0055, USA

ARTICLE INFO

Article history:
Received 24 September 2018
Received in revised form
7 November 2018
Accepted 9 November 2018
Available online 12 November 2018

Dedicated to Professor Richard J. Puddephatt for his pioneering contributions to the field of organometallic chemistry on the occasion of his 75th birthday.

Keywords:
C-H and C–C bond activation
Lanthanide
Mass-analyzed threshold ionization spectroscopy
Density functional and coupled cluster theory calculations
Reaction mechanism
Laser vaporization molecular beam

ABSTRACT

La atom reactions with 1,4-pentadiene and 1-pentyne are carried out in a laser-vaporization molecular beam source. Both reactions yield a predominant La(C_5H_6) radical from ligand dehydrogenation and a minor La(C_3H_4) species from C–C bond cleavage. The metal-hydrocarbon radicals are characterized with mass-analyzed threshold ionization (MATI) spectroscopy and quantum chemical computations. The MATI spectra of each species formed by the two reactions are essentially identical and consist of a single vibronic band system for La(C_5H_6) and two band systems for La(C_3H_4). Each band system exhibits a strong origin band and several weak vibronic ones. Adiabatic ionization energies, metal-ligand vibrational frequencies, and low-frequency ligand-based modes are measured for the two species. La(C_5H_6) is identified as a six-membered lanthanacycle [La(CHCHCHCHCH$_2$)] (Iso A, C_1), whereas two isomers of La(C_3H_4) are a four-membered metallacycle La(CHCHCH$_2$) (Iso 1, C_1) and a three-membered ring La(CHCCH$_3$) (Iso 2, C_s). The ground electronic state of each radical is a doublet and that of the singly charged cation is a singlet. The remaining two electrons that are associated with the isolated La atom or ion are spin paired in a molecular orbital that is bonding combination between a La 5d orbital and a π^* antibonding orbital of the C_5H_6 or C_3H_4 fragment. For the 1,4-pentadiene reaction, the formation of the six-membered metallacycle La(C_5H_6) involves La addition to a C=C double bond, La insertion into two C(sp^3)–H bonds, and concerted H_2 elimination, whereas the formation of the three- and four-membered La(C_3H_4) rings involves two hydrogen migrations followed by C–C bond breakage to eliminate an ethylene molecule. For the 1-pentyne reaction, the formation of each species requires isomerization of a La(1-pentyne) adduct to a La insertion species and then proceeds with the same elemental steps as those for the diene reaction.

1. Introduction

Hydrocarbon compounds are ubiquitous in nature and could be used as low-cost stock for functionalized organic chemicals, but many of which are too inert to participate in chemical reactions under mild conditions. Transition metal-assisted C–H and C–C bond activation stimulates inert hydrocarbons to react with other molecules and may convert them into value added compounds. Spectroscopic measurements probe state specific energies and structures of short-lived species in the gas phase, which are vital for gaining insight into intrinsic reaction mechanisms and electronic and geometric characteristics for efficient bond activation at metal centers. Such measurements also provide benchmarks to test accuracies of quantum chemical calculations that are complicated by possibly multiple low-energy isomers of each transition metal-containing species and high density of low-lying electronic states of each isomer. Metal ion-hydrocarbon species are largely investigated by infrared or ultraviolet–visible photodissociation or photoelectron spectroscopy [1–15], whereas metal atom-hydrocarbon radicals are mainly studied by resonant two-photon ionization and dispersed fluorescence [16–19], and Fourier transform microwave [20]. We have recently reported the mass-analyzed threshold ionization (MATI) spectroscopy and formation of the metal-hydrocarbon radicals produced by the lanthanide-mediated C–C or C–H bond activation of several small alkenes and alkynes [21–31]. Our studies demonstrate that the

* Corresponding author.
E-mail address: dyang0@uky.edu (D.-S. Yang).

https://doi.org/10.1016/j.jorganchem.2018.11.015
0022-328X/

combination of the MATI spectroscopic measurements with electronic structure calculations is a powerful approach to investigate transient metal-hydrocarbon species.

1,4-pentadiene and 1-pentyne are two of C_5H_8 common isomers. We have recently reported a mass spectrometric and MATI spectroscopic study of a La atom reaction with another C_5H_8 isomer, isoprene (2-methyl-1,3-butadiene) [31]. The mass spectrum of the La + isoprene reaction showed the formation of La(C_nH_m) (n = 2, 3, 5, and 7; m = 2, 4, 6, and 8) through primary and secondary reactions. The primary reactions included molecular association [La(C_5H_8)], dehydrogenation [La(C_5H_6)], and C–C bond cleavage [La(C_2H_2) and La(C_3H_4), whereas the secondary reaction [La(C_7H_8)] involved the addition of a second isoprene molecule to one of the C–C bond cleaved species La(C_2H_2) followed by the loss of H_2. Among these metal-hydrocarbon species, the adduct La(C_5H_8) was by far the most predominant, all other species from the primary reactions were relative minor, and the only species from the secondary reaction was even less. Both isoprene and 1,4-pentadiene possess two C=C double bonds, two C–C single bonds, and eight C–H bonds, but they are not strictly comparable. The former has three C(sp^3) –H bonds and five C(sp^2)–H bonds, while the latter has two and six, respectively. Also, the two single C–C bonds of the 1,4-diene are both sp^2-sp^3 bonds, while in isoprene one is sp^2-sp^3 and the other sp^2-sp^2. Therefore, La reactions with these two diene molecules may yield different products or product distributions. Previously, Peake and Gross studied the Fe^+ reactions with a series of alkynes and alkadienes with collision activated dissociation mass spectrometry and suggested that the alkyne complexes rearranged by insertion of Fe^+ into the propargylic C–C bond, followed by abstraction of a β-H atom from the resulting alkyl fragment [32]. Ni and Harrison investigated reactions of the first row transition metal ions with six C_5H_8 isomers using quadruple cell mass spectrometry [33]. Although late transition ions (Cr^+ -Cu^+) reacted primarily by clustering to give metal-hydrocarbon adducts, the early transition ions (Sc^+, Ti^+ and V^+) showed a high reactivity involving C–H and C–C bond breakages and gave distinctively different mass spectra with each of the C_5H_8 isomers.

This work aims to investigate differences between 1,4-pendadiene and isoprene reactions and possible isomerization between 1,4-pentadiene and 1-pentyne in their reactions with La atom. Photoionization time-of-flight (TOF) mass spectrometry is used to identify masses of reaction products, MATI spectroscopy to probe quantum-state specific energies and molecular structures, and electronic structure calculations to search for possible pathways for the formation of the products. To our knowledge, this is the first vibronic spectroscopic measurements of metal-hydrocarbon radicals formed by any metal atom reactions with 1,4-pentadiene or 1-pentyne.

2. Experimental and computational methods

2.1. Experimental

The metal-cluster beam instrument used in this work consists of reaction and spectroscopy vacuum chambers and was described in a previous publication [34]. The La-hydrocarbon reactions were carried out in a laser-ablation metal cluster beam source. La atoms were generated by Nd:YAG pulsed laser (Continuum Minilite II, 532 nm, ~1.0 mJ/pulse) ablation of a La rod (99.9%, Alfa Aesar) in the presence of a He (99.998%, Scott Gross) carrier gas (40 psi) delivered by a home-made piezoelectric pulsed valve (Physik Instrumente P-286.20). Vapor of 1,4-pentadiene (99%, Aldrich) or 1-pentyne (99%, Aldrich) was introduced 3 cm downstream of the laser ablation point, from which La atoms, He carrier gas, and the hydrocarbon vapor entered a collision tube (2 mm inner diameter, 2 cm length) and were then expanded into the reaction chamber to form a molecular beam. The molecular beam was collimated by a cone-shaped skimmer (2 mm inner diameter) and passed through a pair of deflection plates between which an electric field of 100 V cm^{-1} was applied. Ionic species in the molecular beam that were formed by laser ablation were removed by this electric field, and neutral molecules entered the spectroscopy chamber where they were analyzed by photoionization TOF mass spectrometry.

Prior to the MATI measurements, photoionization efficiency spectra of La-hydrocarbon radicals were recorded to locate an approximate ionization threshold to guide MATI scans. In the MATI experiment, the La-hydrocarbon radicals were excited to high-lying Rydberg states in a single-photon process and ionized by a delayed pulsed electric field. The excitation laser was the frequency doubled output of a tunable dye laser (Lumonics HD-500), pumped by the third harmonic output (355 nm) of a Nd:YAG laser (Continuum Surelite II). The laser beam was collinear and counter propagating with the molecular beam. The ionization pulsed field (320 V cm^{-1}), which was also used for extracting and accelerating ions into the field free region, was generated by two high voltage pulse generators (DEI PVX-4140) and delayed by ~20 μs from the laser pulse by a delayed pulsed generator (SRS DG645). A small dc field (6.0 V cm^{-1}) from another power supply (GW INSTEK GPS-30300) was used to separate the ions produced by direct photoionization from the MATI ions generated by the delayed field ionization. The MATI ion signals were obtained by scanning the tunable dye laser, detected by a dual microchannel plate detector, amplified by a preamplifier (SRS SR445), visualized by a digital oscilloscope (Tektronix TDS 3012), and stored in a laboratory computer. Laser wavelengths were calibrated against titanium atomic transitions in the MATI spectral region [35], and the calibration was done after recording the MATI spectra. The Stark shift on the adiabatic ionization energy (ΔAIE) induced by the dc field (E_f) was calculated using the relation of $\Delta AIE = 6.1E_f^{1/2}$, where E_f is in V cm^{-1} and E is in cm^{-1} [36].

2.2. Computational

Geometry optimization and vibrational frequency calculations were carried out using the Becke's three-parameter hybrid functional with the correlation functional of Lee, Yang, and Parr (B3LYP) and 6-311 + G(d,p) basis set for C and H atoms and the effective-core-potential SDD basis set [37,38] for La. We have extensively used DFT/B3LYP and found this method generally produced adequate results for helping the spectral and structural assignments of the metal-hydrocarbon complexes [39]. No symmetry restrictions were imposed in initial geometry optimizations, but appropriate point groups were used in subsequent optimizations to help identify electronic symmetries. For each optimized stationary point, a vibrational analysis was performed to identify the nature of the stationary point (minimum or saddle point) and to help analyze spectral profile. To refine the energies of the electronic states of La(C_5H_6) and La(C_3H_4), single-point energy calculations were carried out with the coupled cluster with single, double and perturbative triple excitations (CCSD(T)) method. These calculations involved the third-order Douglas-Kroll-Hess scalar relativistic correction and were at the DFT/B3LYP optimized geometries. Basis sets used in the CCSD(T) calculations were cc-pVTZ-DK [40,41] for C and H and cc-pVTZ-DK3 [42] for La. In predicting reaction pathways, minima and transition states were located using the same methodology that was used for geometry optimization. The minima connected by each transition state were confirmed by intrinsic reaction coordinate calculations. The DFT calculations were performed with the Gaussian 09 software package [43], whereas the CCSD(T) calculations were carried out with MOLPRO 2010.1 [44].

To compare with the experimental MATI spectra, multi-dimensional Franck-Condon (FC) factors were calculated from the equilibrium geometries, harmonic vibrational frequencies, and normal coordinates of the neutral and ionized complexes [45]. In these calculations, the recursion relations from Doktorov et al. [46] were employed, and the Duschinsky effect [47] was considered to account for a possible axis rotation from the neutral complex to the cation. Spectral simulations using our homemade software package were obtained using the experimental line width and Lorentzian line shape. Transitions from excited vibrational levels of the neutral complex were considered by assuming thermal excitation at a vibrational temperature where calculated intensities best reproduce observed ones. In comparing simulations with measured spectra, the 0-0 transition in the simulation is aligned with the experimental origin band, but the computed vibrational frequencies are unscaled to directly compare with the measured spectrum.

3. Results and discussion

3.1. TOF mass spectra and La-hydrocarbon species

Fig. 1 displays the TOF mass spectra from La reactions with 1,4-pentadiene and 1-pentyne recorded at 240 nm (5.1660 eV) photoionization. The mass spectra of the two reactions are essentially the same and show a strong La(C_5H_6) peak and a weak La(C_3H_4) peak. La(C_5H_6) is presumably formed by the loss of a H_2 molecule, while La(C_3H_4) by C_2H_4 elimination from 1,4-pentadiene or 1-pentyne. The observation of the same metal-hydrocarbon radicals suggests that the formation of each species may proceed through a common intermediate in the two reactions, or isomerization occurs before the dehydrogenation or C–C cleavage takes place. The major difference between these two C_5H_8 isomers and isoprene is that the former reactions produce predominantly a dehydrogenated species, while the latter yields primarily an association complex [31]. This observation may not be surprising because isoprene is expected to be less reactive due to its bond conjugation. Another difference is that only one C–C cleaved product La(C_3H_4) is observed in the 1,4-pentadiene and 1-pentyne reactions, while two, La(C_3H_4) and La(C_2H_4), are produced from isoprene with a less symmetric carbon skeleton. In addition to the metal-hydrocarbon species, each of the mass spectra shows a strong LaO peak. LaO could be formed by the La reaction with oxygen present in the carrier gas as an impurity or by laser vaporization of LaO impurity in the La rod [21–23,25–31].

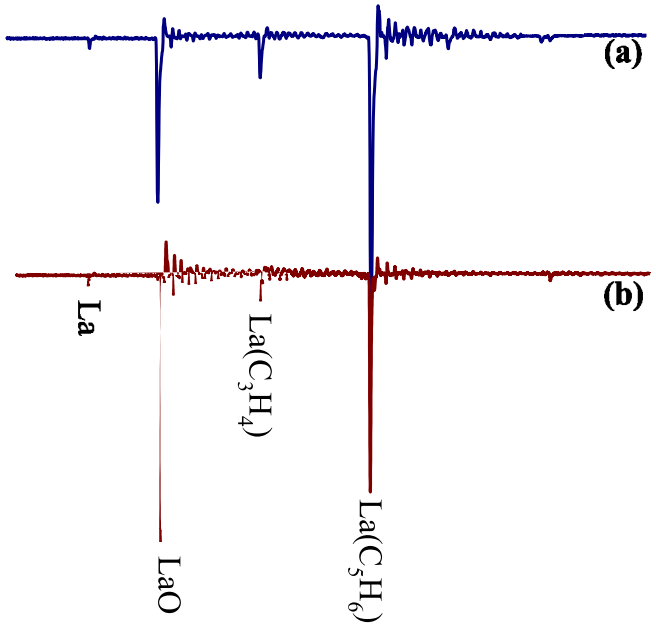

Fig. 1. TOF mass spectra of La reactions with 1,4-pentadiene (a) and 1-pentyne (b) recorded with 240 nm ionization.

3.2. MATI spectra and structural isomers

3.2.1. La(C_5H_6)

Fig. 2 shows the MATI spectra of La(C_5H_6) from the La reactions with 1,4-pentadiene and 1-pentyne. The spectrum of La(C_5H_6) from the 1,4-pentadiene reaction (Fig. 2a) displays the strongest origin band at 37945 (5) cm^{-1}; 321 and 420 cm^{-1} progressions, each with two vibrational quanta, and a weak band at 547 cm^{-1} on the higher energy side of the origin band; and two hot bands at 275 and 362 cm^{-1} below the origin band. Additionally, it exhibits combination bands in the higher energy region that are marked with "*1-*3" and "#1-#3". "*1" and "*2" are combinations of n x 321 + 420 cm^{-1} bands (n = 1 and 2), "*3" is the combination of 321 + 547 cm^{-1} bands, and "#1-#3" are combinations of n x 420 + 547 cm^{-1} (n = 1 and 2) and 420 + 2 × 547 cm^{-1} bands, respectively. The strong origin band and short spectral profile suggest that ionization has a small effect on the molecular geometry. The spectrum of La(C_5H_6) from the 1-pentyne reaction (Fig. 2b) is essentially identical to that from the 1,4-pentadiene reaction in the range of 37800–39000 cm^{-1} where stronger transitions are observed. On the other hand, due to poorer signal to noise ratio, weaker transitions beyond this region was not resolved. Nevertheless, the identical AIE and vibronic bands observed in the

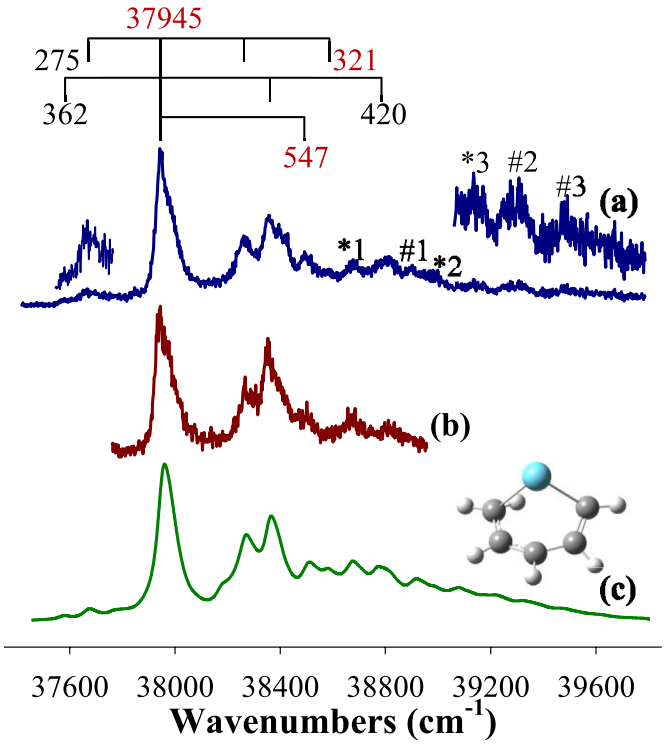

Fig. 2. MATI spectra of La(C_5H_6) from La reactions with 1,4-pentadiene (a) and 1-pentyne (b) and the simulation of the $^1A \leftarrow {}^2A$ transition of La($CH_2CHCHCHCH$) (Iso A) at 200 K (c). MATI bands marked with "*" and "#" are combination bands.

two spectra indicate that the La(C_5H_6) radical formed in the two reactions have the same structures.

Fig. 3 presents the structures of 1,4-pentadiene (a), 1-pentyne (b) and four possible isomers of La(C_5H_6) (c-d). Without going into detailed reaction pathways, Iso A [La($CH_2CHCHCHCH$)] may be considered to be formed from the 1,3- or 3,5-dehydrogenation of 1,4-pentadiene and Iso B [La($CH_2CHCHC(CH_2)$)] from the 2,3- or 3,4-dehydrogenation of the diene molecule, while Iso C [La($CHCCHCH(CH_3)$)] and Iso D [La($CHCCHCH_2CH_2$)] may be formed from the 3,4- and 3,5-dehydrogenations of 1-pentyne, respectively. We have also considered other possible isomers from dehydrogenations of 1,4-pentadiene or 1-pentyne, but our calculations predict that they are significantly higher in energy than the aforementioned isomers. Table 1 lists the molecular point groups, electronic states, and relative energies with vibrational zero-point energy corrections of the two C_5H_8 isomers and four isomers of La(C_5H_6), while Table S1 in Appendix A lists their absolute energies and atomic coordinates. The ground states of the free ligands are singlets; 1,4-pentadiene is predicted to be more stable than 1-pentyne by 9.3 kcal mol^{-1} at the CCSD(T) level, in excellent agreement with the experimental value of 9.1 kcal mol^{-1} from calorimetry measurements [48,49]. The ground states of the four La(C_5H_6) isomers are all doublets with the electron configuration of La $6s^1$, and those of the corresponding ions are singlets produced by removing the La 6s-based electron. The remaining two electrons that are associated with the isolated La atom or ion are spin paired in a molecular orbital that is bonding combination between a La 5d orbital and a π^* antibonding orbital of the C_5H_6 fragment. Thus, the formal oxidation states of La are +2 and + 3 in the neutral and ionized complexes, respectively. To form a quartet state in the neutral complex or a triplet state in the cation, an electron must be excited from a La 5p orbital or a C 2p orbital, and resultant quartet

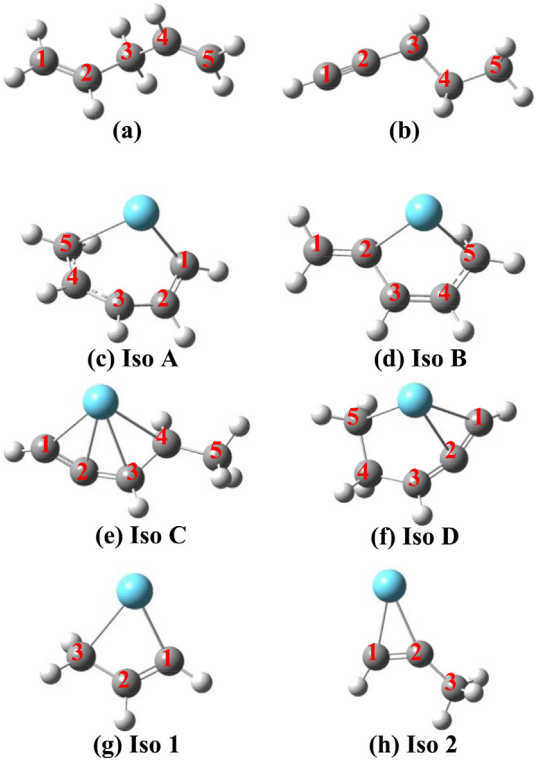

Fig. 3. Structures of 1,4-pentadiene (a), 1-pentyne (b), four isomers of La(C_5H_6) (c–f), and two isomers of La(C_3H_4) (g and h). Relative energies of these isomers are listed in Table 1.

Table 1
Molecular point groups, electronic states, and relative energies (kcal mol^{-1}) of 1,4-pentadiene, 1-pentyne, four isomers of La(C_5H_6), and two isomers of La(C_3H_4) from B3LYP and CCSD(T)//B3LYP calculations. All energies are relative to the energy of the most stable isomers of the free ligand, La(C_5H_6), and La(C_5H_6) and include vibrational zero-point corrections. Energies in parentheses are from CCSD(T)//B3LYP calculations.

Complex	Point Group	State	$E_{B3LYP(CCSD(T))}$
1,4-pentadiene	C_1	^1A	0(0)
1-pentyne	C_s	$^1A'$	10.2(9.3)
La(C_5H_6), Iso A	C_1	^2A	0(0)
	C_1	^1A	110.3(107.4)
La(C_5H_6), Iso B	C_1	^2A	7.4(9.3)
	C_1	^1A	122.4(121.4)
La(C_5H_6), Iso C	C_1	^2A	11.6(11.6)
	C_1	^1A	129.4(126.5)
La(C_5H_6), Iso D	C_1	^2A	15.3(15.7)
	C_1	^2A	131.1(129.1)
La(C_3H_4), Iso 1	C_1	^2A	0(0)
	C_1	^1A	118.7(116.3)
La(C_3H_4), Iso 2	C_s	$^2A'$	2.4(2.6)
	C_s	$^1A'$	120.2(117.5)

or triplet states should have much higher energies than the doublet or singlet. These have been confirmed by our previous studies on La reactions with propene [26], butenes [29], and butynes [28]. Iso A is a six-membered metallacycle with La binding to two terminal carbons (C1 and C5) and more stable (by 9.3 kcal mol^{-1}) than Iso B, a five-membered ring with La binding to C2 and C5. The more stable six-membered ring is likely due to its less strain energy as in the case of cycloalkanes. The higher energy Iso C and Iso D may be described as La(η^4-allenylidene) and La(η^3-allenylidene), respectively. Iso C is slightly more stable (by 4.1 kcal mol^{-1} at the CCSD(T) level) than Iso D because La in Iso C contains one more La–C bond.

The observed MATI spectra in both reactions are assigned to the $^1A \leftarrow {}^2A$ transition of Iso A. This assignment is supported by the excellent agreement between the calculated and observed AIEs, vibrational frequencies, and spectral profiles (Table 2 and Fig. 2). The 321 and 420 cm^{-1} vibronic progressions are assigned to excitations of a La–C1/C5 asymmetric stretch (ν_{27}^+) and a C1–C2–C3 in-plane bend (ν_{26}^+) in the ion, while the 547 cm^{-1} band is assigned to the excitation of a La–C5 stretch coupled with a terminal CH_2 rock (ν_{24}^+) in the ion. The hot bands at 275 and 362 cm^{-1} are due to thermal excitations of the La–C1/C5 asymmetric stretch (ν_{27}) and the C1–C2–C3 in-plane bend (ν_{26}) in the neutral state, respectively. The vibrational temperature of the La(C_5H_6) is estimated to be ~200 K based on the intensities of the hot bands relative to that of the origin band. The observation of a strong origin band and weaker vibronic transitions is consistent with the theoretical predictions of similar neutral and ion geometries (Table S2). We have also considered possible contributions of Iso B, C, and D to the MATI spectra, but they are excluded due to large errors in computed AIEs of these isomers (Table 1) and mismatched spectral simulations (Figure S1). The calculated AIEs of Iso B, C, and D at the CCSD(T) level are 40246, 41251, and 40527 cm^{-1}, each is considerably higher than the measured value of 37945 cm^{-1}.

3.2.2. La(C_3H_4)

Fig. 4 presents the MATI spectra of La(C_3H_4) formed from the 1,4-pentadiene and 1-pentyne reactions. The two spectra are essentially identical to each other, indicating that the spectral carriers are the same in two cases. Previously, we studied MATI spectra of La(C_3H_4) produced by La + propene and La + isoprene reactions and identified two isomers from the propene reaction and one from isoprene [26,31]. The current spectra are like that of the propene-dehydrogenated La(C_3H_4) though the MATI signals are weaker

Table 2
Adiabatic ionization energies (AIEs, cm^{-1}) and vibrational frequencies (cm^{-1}) of La(C_5H_6) (Iso A), and La(C_3H_4) (Iso 1 and Iso 2) from MATI spectra and B3LYP and CCSD(T)//B3LYP calculations. ν_n^+ and ν_n are vibrational modes in the ionic and neutral states, and the energies in parentheses are from CCSD(T)//B3LYP calculations.

Complex	MATI	B3LYP [CCSD(T)]	Mode description[a]
La(C_5H_6) (Iso A), C_1, $^1A \leftarrow {}^2A$			
AIE	37945	38591(37571)	
ν_{27}^+/ν_{27}	321/275	313/282	La–C1/C5 asymmetric stretch
ν_{26}^+/ν_{26}	420/362	407/376	C1–C2–C3 in-plane bend
ν_{24}^+	547	553	La–C5 stretch & CH_2 rock
La($CHCHCH_2$) (Iso 1), C_1, $^1A \leftarrow {}^2A$			
AIE	40942	41540(40711)	
ν_{18}^+	140	156	C–C–C out-of-plane bend
ν_{16}^+	362	362	La–C2/C3 stretch
ν_{15}^+	414	451	La–C1/C2 stretch & CH_2 rock
La($CHCCH_3$) (Iso 2), C_s, $^1A' \leftarrow {}^2A'$			
AIE	40509	41214(40216)	
ν_{11}^+	433	442	La–C2 stretch & C2–CH_3 in-plane bend
ν_{10}^+	572	570	La–C1 stretch & C1–H in-plane bend

[a] Carbon atomic numbering is shown in Fig. 3.

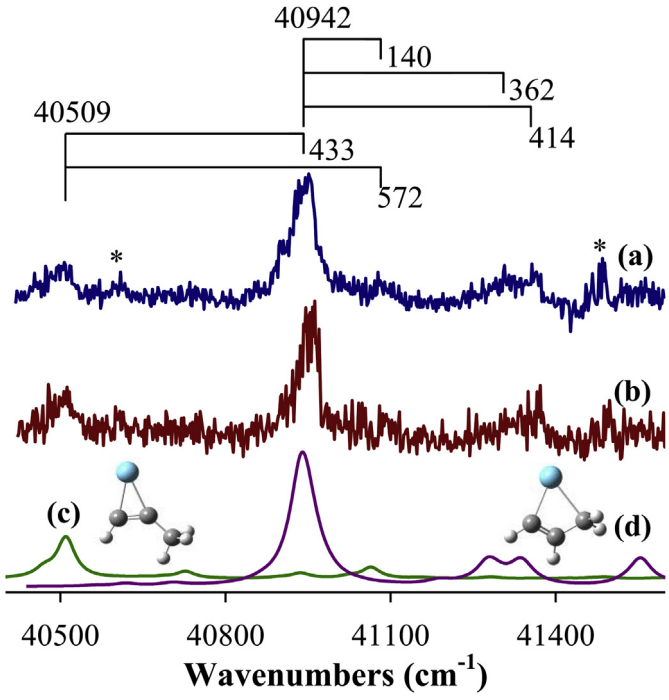

Fig. 4. MATI spectra of La(C_3H_4) from La reactions with 1,4-pentadiene (a) and 1-pentyne (b) and simulations of the $^1A \leftarrow {}^2A$ transition of La($CHCHCH_2$) (Iso 1) (c) and the $^1A' \leftarrow {}^2A'$ transition of La($CHCCH_3$) (Iso 2) (d) at 300 K. MATI bands marked with "*" are from ionization of LaO.

due to the low number density of the species produced in these C–C cleavage reactions. Thus, the current spectra can easily be assigned to two band systems from ionization of two isomers (Fig. 3g and h) by comparing with spectral simulations (Fig. 4c and d) and the MATI spectra of La(C_3H_4) from the La + propene reaction. The 40942 cm^{-1} band system consisting of the origin band at 40942 cm^{-1} and three weak bands at 140, 362 and 414 cm^{-1} is assigned to the $^1A \leftarrow {}^2A$ transition of La($CHCHCH_2$) (Iso 1), while the 40509 cm^{-1} band system consisting of the origin band at 40509 cm^{-1} and two weak bands at 433 and 572 cm^{-1} is attributed to the $^1A' \leftarrow {}^2A'$ transition of La($CHCCH_3$) (Iso 2). Like La(C_5H_6), the doublet state of each isomer of La(C_3H_4) has a La $6s^1$ valence electron configuration, and the singlet ion is formed by removing the $6s^1$ electron. The weaker signal of the 40509 band systems is consistent with the predicted higher energy of Iso 2. The 140, 362, and 414 cm^{-1} bands are assigned to a C–C–C out-of-plane bend (ν_{18}^+), a La–C2/C3 stretch (ν_{16}^+), and a La–C1/C2 stretch combined with a CH_2 rock (ν_{15}^+) of Iso 1, while the 433 and 572 cm^{-1} bands are attributed to the La–C2 stretch combined with a C2–CH_3 in-plane bend (ν_{11}^+) and a La–C1 stretch mixed with a C1–H in-plane bend (ν_{10}^+) of Iso 2. It is noted that the 433 and 572 cm^{-1} bands from Iso 2 are overlapped with the origin and 140 cm^{-1} bands of Iso 1, respectively. The observed AIEs and vibrational frequencies are compared with computed values in Table 2. For the AIEs, the CCSD(T) values are 200–300 cm^{-1} smaller than the measured values, while the B3LYP values are 600–700 cm^{-1} larger. The computed differences between the AIEs of the two isomers are 495 cm^{-1} at the CCSD(T) level and 326 cm^{-1} at the B3LYP level, while the measured AIE difference is 433 cm^{-1}. For the vibrational frequencies, a reasonable agreement also exists between the calculations and measurements. In addition to the aforementioned vibronic bands, the spectra also exhibit two other bands marked with "*", which are from the ionization of LaO as discussed previously [26,31].

3.3. Formation of La(C_5H_6) and two isomers of La(C_3H_4)

Figs. 5 and 6 present the DFT/B3LYP computed stationary points for the formation of Iso A of La(C_5H_6) and two isomers of La(C_3H_4) from the La + 1,4-pentadiene reaction, whereas Fig. 7 illustrates the stationary points for the formation of HLa($CH_2CHCHCH_2$) (IM3) from La + 1-pentyne. These stationary points include reactants, intermediates (IMn), transition states (TSn), and products in their doublet spin states. Energies of the stationary points reported in these figures are all electronic energies with vibrational zero-point corrections, which are also reported in Tables S3 and S4 of Appendix A. We have also carried out CCSD(T) singlet-point energy calculations for the stationary points for the formation of La(C_5H_6) (Iso A) from the La + 1,4-pentadiene reaction. The CCSD(T) energies are compared with those from the DFT/B3LYP calculations in Table S5, and the comparison shows that the relative energies from the two calculations are only slightly different (by 0.1–1.0 kcal mol^{-1}). Because of the similarly relative energies and high computational cost, the CCSD(T) calculations were not performed for the stationary points for the formation of the two La(C_3H_4) isomers from the La +1,4-pentadiene reaction and for the formation of La(C_5H_6) and La(C_3H4) from the La + 1-pentyne reaction.

3.3.1. Formation of La(C_5H_6) and two isomers of La(C_3H_4) from La + 1,4-pentadiene

The formation of Iso A of La(C_5H_6) from the La + 1,4-pentadiene reaction (Fig. 5) involves La addition to a C=C double bond, La insertion into two C(sp^3)–H single bonds, and concerted H_2 elimination. La addition to a C=C bond forms a π complex (IM1). Upon the La addition, the C1C2 bond is elongated (from 1.331 to 1.513 Å) and the ethenyl plane of the ligand is bent. This structural change suggests that the π bond is broken between the C1 and C2 atoms and the two carbon atoms rehybridize from sp^2 to sp^3. Thus, IM1 can be considered a three-membered metallacycle. The breakage of the C–C π bond is over compensated by the formation of two La–C bonds and the resultant metallacycle is more stable than the isolated reactants by 32.6 kcal mol^{-1} (Table S3). The stabilization energy of La addition to 1,4-pentadiene is similar to those of La associations with other small alkenes (ethylene, propene, and butenes) [23,26,27,29]. The reaction could also begin by La addition to two C=C double bonds of the ligand. However, the double addition requires the trans-cis isomerization of the ligand, and the resultant π complex is less stable than IM1 by 6.7 kcal mol^{-1}. The second step is the activation of two C(sp^3)–H bonds by La insertion (IM1-IM3). Prior to La insertion, the CH_2=CH– group rotates around the C3–C4 single bond to form IM2, which facilitates the β C–H bond insertion and the formation of the inserted species IM3. Unlike IM2, the carbon skeleton in IM3 is nearly planar, suggesting that carbon p_π electrons are delocalized over all five carbons. The electron delocalization, the La η^5 binding mode with the five carbons, and the formation of the La–H bond makes IM3 more stable than IM2 even though a C–H bond is broken from IM2 to IM3. Because of the electron delocalization, The C–C bond lengths become very comparable (1.425 ± 0.005 Å), the carbons in all C–H bonds have similar orbital hybridization characters, and IM3 possesses a reflection plane (i.e., HLaC3H). The second La insertion occurs at a terminal C–H bond (C1–H or C5–H) with H pointing inwards and yields a dihydrogen complex (IM4). IM4 is a dihydrogen complex rather than a dihydride species because the H–H distance (0.757 Å) is about the same as that in a free H_2 molecule. The elimination of H_2 produces Iso A. The whole process La + 1,4-pentadiene → Iso + H_2 is exothermic by 42.6 kcal mol^{-1} and has no energy barriers. We have also considered possibilities of La insertion into the C3–H and C2–H (or C4–H) bonds because all C–H bonds are comparable in their bond strengths (Figure S2). However, our calculations show that La insertions into either C3–H (blue trace) or C2–H (or C4–H) (red trace) bonds are kinetically less favorable than La insertion into the C1–H (or C5–H) bond (black trace) because of their higher barriers. Moreover, the five-membered ring (Iso B) from La insertion into the C2–H (or C4–H) bond and the four-membered ring from La insertion into the C3–H bond are less stable than Iso A from the C1–H (or C5–H) insertion.

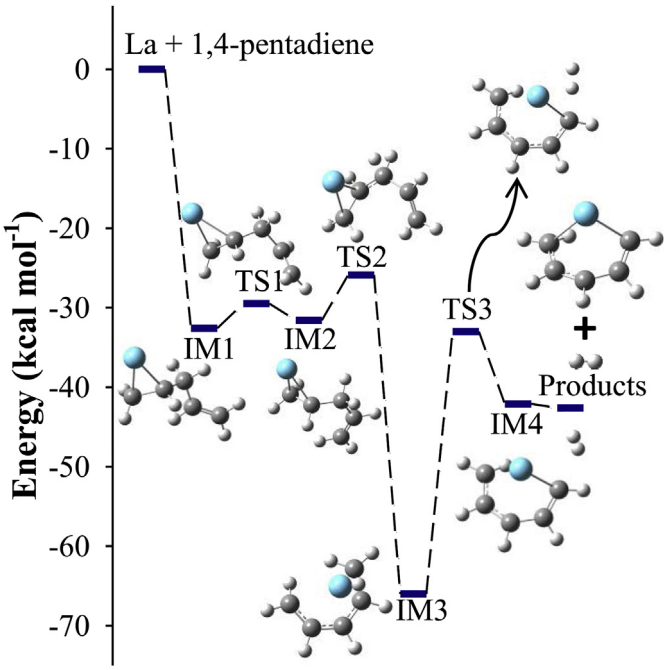

Fig. 5. Reaction pathway and energy profile for the formation of La($CH_2CHCHCHCH$) (Iso A) from the La + 1,4-pentadiene reaction calculated at the DFT/B3LYP level, where IMn stands for intermediates and TSn transition states.

The formation of the two isomers of La(C_3H_4) from La + 1,4-pentadiene is illustrated in Fig. 6. Previously, we investigated La-mediated C–C bond cleavage of propene [27], butadiene [25], isoprene [31], and 1- and 2-pentene [30], and found that the C–C cleavage could proceed via hydrogen migration followed by C–C cleavage or vice versa. The formation of La(CH_2) in the La + propene reaction, La(C_2H_2) in La + 1,3-butadiene, and La(C_2H_2) and La(C_3H_4) in La + isoprene all follows the mechanism of hydrogen migration prior to C–C bond cleavage, while the formation of La(C_2H_2) in the La + 1- and 2-pentene reactions proceeds with an opposite order. In the La + 1,4-pentadiene reaction, the formation of La(C_3H_4) Iso 1 is through hydrogen migration from C3 to C2, followed by C2–C3 bond cleavage and ethylene elimination, and that of Iso 2 requires two hydrogen migrations from C3 to C5 and C4 to C2 prior to the C2–C3 cleavage and ethylene elimination. In both cases, the reaction begins with La addition to a C=C bond and insertion into the C3(sp^3)–H bond (i.e., La + 1,4-pentadiene → IM1 → IM2 → IM3) as discussed in the previous paragraph. To form Iso 1, the La-bonded H in IM3 is migrated to C2 to form a four-membered lanthanacycle La($CH_2CH_2CHCHCH_2$) (IM5). In this four-membered ring, La is bonded with C1 and C3, the two C–C bonds inside the ring are single bonds (1.545 and 1.572 Å), and the two C–C bonds outside the ring are between single and double bonds (1.397 and 1.410 Å). IM5 is less stable than IM3 due to the partial loss of the C 2p electron delocalization (from over 5 carbons to 3 carbons) and the La–C bonding (from η^5 to η^2). Because it is weaker than the C3=C4 double bond, C–C cleavage occurs preferably at the C2–C3 single bond to form (C_2H_4)La($CHCHCH_2$) (IM6). Because the singlet C_2H_4 molecule has much weaker bonding with La than the $CHCHCH_2$ radical does, IM6 favors decomposition into La($CHCHCH_2$) + C_2H_4. The formation of Iso 2 requires several more steps as it involves two H migration. The first H migration from the La-bonded H in IM3 to C5 forms a five-membered ring, La($CH_2CHCHCHCH_3$) (IM7). The second H migration from C4 to C2 involves La insertion into a C4(sp^3)–H bond to form an inserted species (IM8) and the La-bonded H migrates to C5 to form another five-membered ring (IM9). Although both are five-membered rings, IM7 is considerably more stable than IM9 (by 12.8 kcal mol^{-1}). This stability difference largely arises from their different conformations. IM7 is puckered as an envelope shape that minimizes torsional strain compared to the less puckered IM9 with higher strain energy. In IM9, C1–C2, C2–C3, and C4–C5 are all single bonds, while C3=C4 is a double bond. Although breaking any of the C–C single bonds would be possible, the C2–C3 bond cleavage produces a singlet ethylene molecule and a La($CHCCH_3$) radical (Iso 2), which is thermodynamically more favorable than cleaving C1–C2 or C4–C5 bonds that would yield two radicals (a hydrocarbon fragment and a metal-hydrocarbon complex). We have also considered the formation of the two La(C_3H_4) isomers in a reversed sequence (i.e. C–C cleavage prior to dehydrogenation). However, the reversed reaction order is less favorable because the C2=C3 bond in either IM3 or IM7 requires more energy to cleave than the C2–C3 single bond in IM5 or IM9.

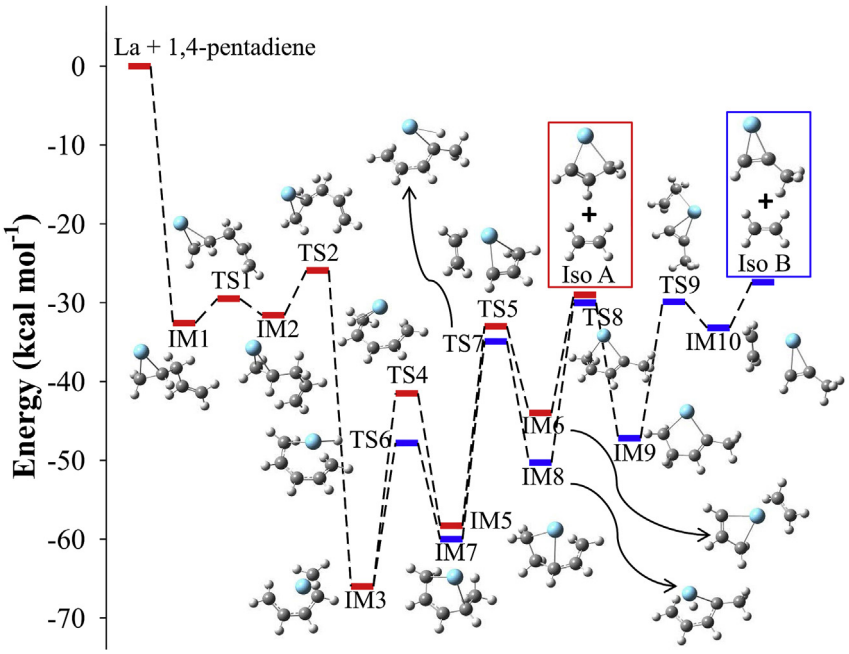

Fig. 6. Reaction pathway and energy profile for the formation of La(CHCHCH$_2$) (Iso 1) and La(CHCCH$_3$) (Iso 2) from the La + 1,4-pentadiene reaction calculated at the DFT/B3LYP level, where IMn stands for intermediates and TSn transition states.

The formation of the La(C_3H_4) two isomers from La + 1,4-pentadiene are thermodynamically and kinetically favorable. The formation of Iso 1 is predicted to be exothermic by 29.9 kcal mol^{-1} and that of Iso 2 by 27.4 kcal mol^{-1}. But both are significantly less exothermic than the formation of La(C_5H_6) (42.6 kcal mol^{-1}). The computational predictions agree with the mass spectra that show a much stronger La(C_5H_6) signal than La(C_3H_4). Moreover, because Iso 2 is less stable and produced through more reaction steps than Iso 1, the number density of Iso 2 is lower as shown by its MATI signal.

3.3.2. *Formation of La(C_5H_6) and two isomers of La(C_3H_4) from La + 1-pentyne*

Unlike 1,4-pentadiene, simple dehydrogenation of 1-pentyne could not produce La(C_5H_6) (Iso A) because the free ligand (CHCCH$_2$CH$_2$CH$_3$) and the hydrocarbon fragment (CHCHCHCHCH$_2$) in La(C_5H_6) have different atomic connectivity. To form the metal complex, isomerization must occur through hydrogen migration either before or after metal coordination. However, hydrogen migration without metal assistance is expected to have a considerable energy barrier. Isomerization of 1-pentyne to 1,4-pentadiene is unlikely in our experiments for the ligand is introduce to the collision chamber at ambient temperatures and without passing through the laser ablation region. Our calculations show that the isomerization proceeds via La addition to 1-pentyne to form La(1-pentyne), which then converts to IM3. Upon the formation of IM3, La + 1-pentyne → La(C_5H_6) (Iso A) + H_2 follows the same path as that of the La + 1,4-pentadiene reaction discussed in Section 3.3.1. Thus, we will only describe the formation and isomerization of La(1-pentyne) (Fig. 7).

La addition to the triple bond in 1-pentyne forms a π-complex (IM11). Upon the La addition, the C≡C triple bond is elongated (from 1.20 to 1.35 Å) and the C(sp)–H bond is bent away from the H–C≡C- linear configuration. Thus, the π complex may be considered a propyl substituted lanthanacyclopropene. The resultant three-membered ring is lower in energy than the La + 1-pentyne reactants by 54.4 kcal mol^{-1} (Table S4). The stabilization energy is similar to those of La additions to propyne (54.4 kcal mol^{-1}) [21], 1-butyne (52.4 kcal mol^{-1}) [28], 2-butyne (51.1 kcal mol^{-1}) [28], but it is considerably larger than that of La + 1,4-pentadiene (32.4 kcal mol^{-1}). As a result, IM11 is more stable than La(1,4-pentadiene) (IM1) even though 1-pentyne is less stable than the diene molecule. Alkynes are generally better electrophiles due to their lower-energy empty C pπ orbitals and tend to have stronger back electron donations than alkenes, which lead to shorter La–C bonds (2.294/2.325 Å) in IM11 than those in IM1 (2.367/2.372 Å). Isomerization of IM11 to IM3 requires two H migrations, each followed by the formation of a metallacycle. The first H migration from C3 to C2 (IM11-IM15) forms La(CHCHCHCH$_2$CH$_3$) (IM15), a metal-carbene complex with La doubly bound to C1. To facilitate the C3, C2–H migration, the propyl group in IM11 rotates to bring one of the H atoms in the β position (i.e. C3) to the proximity of the La atom (IM12) to enhance the La and H interaction. Such interaction weakens the C–H bond (as shown by the elongation of the C–H bond from 1.100 Å in IM11 to 1.271 Å in IM12) and promotes the La–H bond formation (IM13). IM12 is less stable than IM11 due to the weakened C–H bond, while IM13 is more stable than IM12 due to the formation of new C2=C3 and La–H bonds, which overcompensates the loss of a La–C bond. The La–H bond in IM13 rotates to bring the H atom to the vicinity of the C2 atom (IM14) to facilitate the H transfer from La to C2 (IM15). Therefore, the C3,C2–H migration consists of two steps with H migration from C3 to La and then from La to C2. The second H migration from C4 to C1 is like the first H shift from C3 to C2. It begins with the formation of a four-membered metallacycle (IM16), proceeds with H shift from C4 to La (IM17), and completes with H migration from La to C1 (IM18). Finally, IM3 is formed via a five-membered lanthanacycle intermediate (IM19). The La + 1-pentyne → IM3 process is exothermic by 76.2 kcal mol^{-1} and has no positive barriers.

We have also considered the possible isomerization of La(1-pentyne) to other intermediates along the La + 1,4-pentadiene → La(C_5H_6) (Iso A) + H_2 reaction coordinates and Iso C or Iso D to Iso A. However, all these alternatives are less favorable than La + 1-pentyne → IM3 → La(C_5H_6) (Iso A) + H_2 discussed above. For

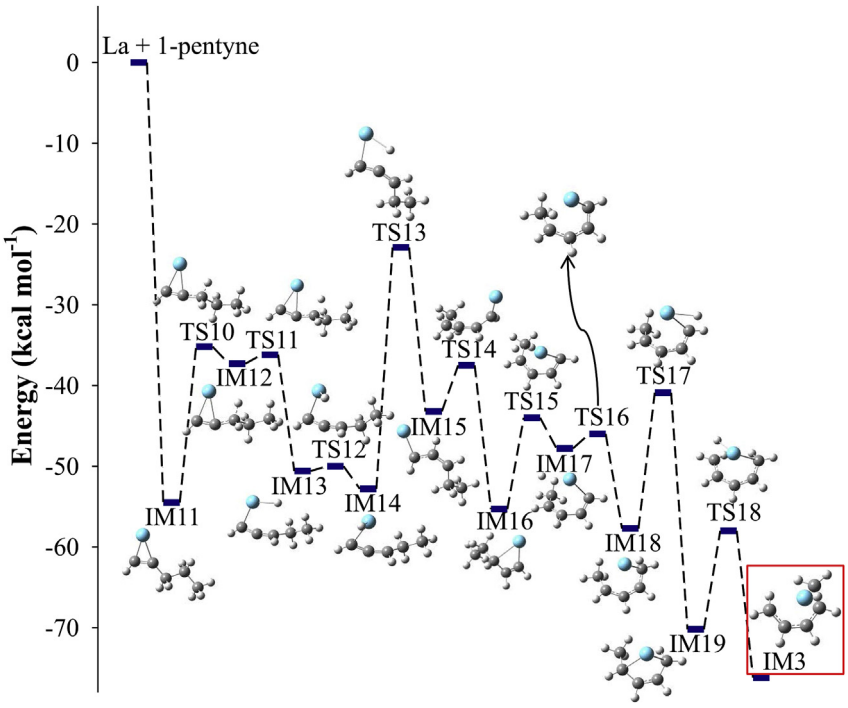

Fig. 7. Reaction pathway and energy profile for the formation of the H–La($CH_2CHCHCHCH_2$) (IM3) from the La + 1-pentyne reaction calculated at the DFT/B3LYP level, where IMn stands for intermediates and TSn transition states.

example, La + 1-pentyne → IM2 is predicted to have an energy barrier of 5.9 kcal mol^{-1} (Figure S3 and Table S4), while the isomerization of Iso C and Iso D have barriers up to 33.0 and 28.8 kcal mol^{-1}, respectively (Figure S4 and Table S4).

IM3 is the key intermediate for the formation of Iso 1 and Iso 2 of La(C_3H_4) in the 1,4-pentadiene reaction and Iso A of La(C_5H_6) in both 1,4-pentadiene and 1-pentyne reactions. It is also the most stable intermediate in these reactions (Figs. 5–7). Thus, it is not unreasonable to assume that IM3 could also be an intermediate for the formation of the two La(C_3H_4) isomers in the La + 1-pentyne reaction, and from IM3 the C–C cleavage of 1-pentyne follows the same paths as those illustrated in Fig. 6. The main difference is that the exothermicity in the formation of the two La(C_3H_4) isomers is slightly larger for 1-pentyne (40.1 kcal mol^{-1} for Iso 1 and 37.6 kcal mol^{-1} for Iso 2) than for 1,4-pentadiene (29.9 kcal mol^{-1} for Iso 1 and 27.4 kcal mol^{-1} for Iso 2).

4. Conclusions

La atom reactions with 1,4-pentadiene and 1-pentyne in the gas phase show dehydrogenation to be the main reaction channel and ethylene elimination the minor one. Both reactions produce La(C_5H_6) from the dehydrogenation and La(C_3H_4) from the C–C bond cleavage. La(C_5H_6) is identified as a six-membered metallacycle in C_1 point group. Two isomers of La(C_3H_4) are observed as a four-membered metallacycle La($CHCHCH_2$) in C_1 pointe group and a three-membered ring La($CHCCH_3$) in C_s. The ground electronic state of each species is a doublet with a La $6s^1$-based electron configuration, and ionization of the neutral state yields a singlet state in a similar geometry. For the La + 1,4-pentadiene reaction, La(C_5H_6) is formed via concerted H_2 elimination, whereas the formation of the La(C_3H_4) two isomers involves the two H migrations, C–C bond cleavage, and ethylene elimination. For the La + 1-pentyne reaction, the formation of La(C_5H_6) and La(C_3H_4) requires the isomerization of a La(1-pentyne) adduct to a La inserted species in addition to those for the La + 1,4-pentadiene reaction.

Acknowledgments

We are grateful for the financial support from the National Science Foundation Division of Chemistry (Chemical Structure, Dynamics, and Mechanisms, Grant No. 1800316).

Appendix A. Supplementary data

Supplementary data to this article can be found online at https://doi.org/10.1016/j.jorganchem.2018.11.015.

References

[1] R.S. Walters, T.D. Jaeger, M.A. Duncan, Infrared spectroscopy of $Ni^+(C_2H_2)_n$ complexes: evidence for intracluster cyclization reactions, J. Phys. Chem. A 106 (44) (2002) 10482–10487.
[2] R.S. Walters, E.D. Pillai, P.v.R. Schleyer, M.A. Duncan, Vibrational spectroscopy and structures of $Ni^+(C_2H_2)_n$ (n=1-4) complexes, J. Am. Chem. Soc. 127 (2005) 17030–17042.
[3] R.S. Walters, P.V. Schleyer, C. Corminboeuf, M.A. Duncan, Structural trends in transition metal cation-acetylene complexes revealed through the C-H stretching fundamentals, J. Am. Chem. Soc. 127 (4) (2005) 1100–1101.
[4] A.D. Brathwaite, T.B. Ward, R.S. Walters, M.A. Duncan, Cation-π and CH-π interactions in the coordination and solvation of Cu^+(acetylene)$_n$ complexes, J. Phys. Chem. A 119 (22) (2015) 5658–5667.
[5] M. Citir, G. Altinay, G. Austein-Miller, R.B. Metz, Vibrational spectroscopy and theory of $Fe^+(CH_4)_n$ (n=1-4), J. Phys. Chem. A 114 (42) (2010) 11322–11329.
[6] A. Kocak, M.A. Ashraf, R.B. Metz, Vibrational spectroscopy reveals varying structural motifs in $Cu^+(CH_4)_n$ and $Ag^+(CH_4)_n$ (n=1-6), J. Phys. Chem. 119 (2015) 9653–9665.
[7] A. Kocak, Z. Sallese, M.D. Johnston, R.B. Metz, Vibrational spectroscopy of $Co^+(CH_4)_n$ and Ni^+ $(CH_4)_n$ (n=1-4), J. Phys. Chem. A 118 (18) (2014) 3253–3265.
[8] M.A. Ashraf, C.W. Copeland, A. Kocak, A.R. McEnroe, R.B. Metz, Vibrational spectroscopy and theory of $Fe_2^+(CH_4)_n$ (n=1-3), Phys. Chem. Chem. Phys. 17 (2015) 25700–25704.
[9] C.W. Copeland, M.A. Ashraf, E.M. Boyle, R.B. Metz, Vibrational spectroscopy of $Fe_3^+(CH_4)_n$ (n = 1-3) and $Fe_4^+(CH_4)_4$ J, Phys. Chem. A 121 (10) (2017) 2132–2137.
[10] V.J.F. Lapoutre, B. Redlich, A.F.G. van der Meer, J. Oomens, J.M. Bakker, A. Sweeney, A. Mookherjee, P.B. Armentrout, Structures of the dehydrogenation products of methane activation by 5d transition metal cations, J. Phys. Chem. 117 (2013) 4115–4126.

[11] O.W. Wheeler, M. Salem, A. Gao, J.M. Bakker, P.B. Armentrout, Activation of C-H bonds in $Pt^+ + x\ CH_4$ reactions, where x=1-4: identification of the platinum dimethyl cation, J. Phys. Chem. A 120 (31) (2016) 6216–6227.

[12] S.R. Miller, T.P. Marcy, E.L. Millam, D.G. Leopold, Photoelectron spectroscopic characterization of the niobium-benzene anion produced by reaction of niobium with ethylene, J. Am. Chem. Soc. 129 (12) (2007) 3482–3483.

[13] W.Y. Lu, P.D. Kleiber, M.A. Young, K.H. Yang, Photodissociation spectroscopy of $Zn^+(C_2H_4)$, J. Chem. Phys. 115 (13) (2001) 5823–5829.

[14] A.S. Gentlman, A.E. Green, D.R. Price, E.M. Cunningham, A. Iskra, S.R. Mackenzie, Infrared spectroscopy of $Au^+(CH_4)_n$ complexes and vibrationallyy-enhanced C-H activation reactions, Top. Catal. 61 (1–2) (2018) 81–91.

[15] J.A. Maner, D.T. Mauney, M.A. Duncan, Imaging charge transfer in a cation-π system: velocity-map imaging of Ag^+(benzene) photodissociation, J. Phys. Chem. Lett. 6 (22) (2015) 4493–4498.

[16] D.J. Brugh, R.S. Dabell, M.D. Morse, Vibronic spectroscopy of unsaturated transition metal complexes: CrC_2H, $CrCH_3$, and $NiCH_3$, J. Chem. Phys. 121 (2004) 12379–12385.

[17] M.A. Garcia, M.D. Morse, Electronic spectroscopy and electronic structure of copper acetylide, CuCCH, J. Phys. Chem. A 117 (39) (2013) 9860–9870.

[18] D.J. Brugh, M.D. Morse, Rotational analysis of the 3_0^1 band of the A ^{6}sigma$^+$ - X ^{6}sigma$^+$ system of CrCCH, J. Chem. Phys. 141 (2014), 064304.

[19] E.L. Johnson, M.D. Morse, The (A)over-tilde(2) Delta(5/2) <- (X)over-tilde(2) Delta(5/2) electronic band system of nickel acetylide, NiCCH, Mol. Phys. 113 (15–16) (2015) 2255–2266.

[20] M.A. Flory, A.J. Apponi, L.N. Zack, L.M. Ziurys, Activation of methane by zinc: gas-phase synthesis, structure, and bonding of $HZnCH_3$, J. Am. Chem. Soc. 132 (48) (2010) 17186–17192.

[21] D. Hewage, M. Roudjane, W.R. Silva, S. Kumari, D.-S. Yang, Lanthanum-mediated C-H bond activation of propyne and identification of $La(C_3H_2)$ isomers, J. Phys. Chem. 119 (2015) 2857–2862.

[22] D. Hewage, W.R. Silva, W. Cao, D.-S. Yang, La-activated bicyclo-oligomerization of acetylene to naphthalene, J. Am. Chem. Soc. 138 (2016) 2468–2471.

[23] S. Kumari, W. Cao, Y. Zhang, M. Roudjane, D.-S. Yang, Spectroscopic characterization of lanthanum-mediated dehydrogenation and C-C bond coupling of ethylene, J. Phys. Chem. 120 (2016) 4482–4489.

[24] Y. Zhang, M.W. Schmidt, S. Kumari, M.S. Gordon, D.-S. Yang, Threshold ionization and spin-orbit coupling of ceracyclopropene formed by ethylene dehydrogenation, J. Phys. Chem. 120 (2016) 6963–6969.

[25] D. Hewage, W. Cao, J.H. Kim, Y. Wang, Y. Liu, D.-S. Yang, Spectroscopic characterization of nonconcerted [4+2] cycloaddition of 1,3-butadiene with lanthanacyclopropene to form lanthanum-benzene in the gas phase, J. Phys. Chem. A 121 (2017) 1233–1239.

[26] S. Kumari, W. Cao, D. Hewage, R. Silva, D.-S. Yang, Mass-analyzed threshold ionizaiton spectroscopy of lanthanum-hydrocarbon radicals formed by C-H bond activation of propene, J. Chem. Phys. 146 (2017), 074305.

[27] D. Hewage, W. Cao, S. Kumari, R. Silva, T.H. Li, D.-S. Yang, Spectroscopic and formation of lanthanum-hydrocarbon radicals formed by C-C bond cleavage and coupling of propene, J. Chem. Phys. 146 (2017), 184304.

[28] W. Cao, D. Hewage, D.-S. Yang, Lanthanum-mediated dehydrogenation of 1- and 2-butynes: spectroscopy and formation of $La(C_4H_4)$ isomers, J. Chem. Phys. 147 (2017), 064303.

[29] W. Cao, D. Hewage, D.-S. Yang, Lanthanum-mediated dehydrogenation of butenes: spectroscopy and formation of $La(C_4H_6)$ isomers, J. Chem. Phys. 148 (2018), 044312.

[30] W. Cao, Y. Zhang, S. Nyambo, D.-S. Yang, Spectroscopy and formation of lanthanum-hydrocarbon radicals formed by C-H and C-C bond activation of 1-pentene and 2-entene, J. Chem. Phys. 149 (2018), 034303.

[31] W. Cao, D. Hewage, D.-S. Yang, Spectroscopy and formation of lanthanum-hydrocarbon radicals formed by association and carbon-carbon bond cleavage of isoprene, J. Chm. Phys. 148 (2018), 194302.

[32] D.A. Peake, M.L. Gross, Reaction of gas-phase iron(I) with alkynes and dienes: mechanism of rearrangement after insertion into propargylic or allylic carbon-carbon bonds, Organometallics 5 (6) (1986) 1236–1243.

[33] J.S. Ni, A.G. Harrison, Reactive collisions in quadrupole cells .7. Characterization of C_5H_8 isomers by reaction with metal ions, Rapid Commun. Mass Spectrom. 10 (2) (1996) 220–224.

[34] B.R. Sohnlein, S.G. Li, J.F. Fuller, D.-S. Yang, Pulsed-field ionization electron spectroscopy and binding energies of alkali metal dimethyl ether and dimethoxyethane complexes, J. Chem. Phys. 123 (1) (2005), 014318.

[35] C.E. Moore, Atomic Energy Levels, National Bureau Standards, Washington, DC, 1971.

[36] M.A. Duncan, T.G. Dietz, R.E. Smalley, Two-color photoionization of naphthalene and benzene at threshold, J. Chem. Phys. 75 (5) (1981) 2118–2125.

[37] X. Cao, M. Dolg, Valence basis sets for relativistic energy-consistent small-core lanthanide pseudopotentials, J. Chem. Phys. 115 (16) (2001) 7348–7355.

[38] X. Cao, M. Dolg, Segmented contraction scheme for small-core lanthanide pseudopotential basis sets, J. Mol. Struc.-Theochem. 581 (1–3) (2002) 139–147.

[39] D.-S. Yang, High-resolution electron spectroscopy of gas-phase metal-aromatic complexes, J. Phys. Chem. Lett. 2 (1) (2011) 25–33.

[40] T.H. Dunning Jr., Gaussian basis sets for use in correlated molecular calculations. I. The atoms boron through neon and hydrogen, J. Chem. Phys. 90 (1989) 1007–1023.

[41] W.A. de Jong, R.J. Harrison, D.A. Dixon, Parallel Douglas–Kroll energy and gradients in NWChem: estimating scalar relativistic effects using Douglas–Kroll contracted basis sets, J. Chem. Phys. 114 (2001) 48–53.

[42] Q. Lu, K.A. Peterson, Correlation consistent basis sets for lanthanides: the atoms La-Lu, J. Chem. Phys. 145 (2016), 054111.

[43] M.J. Frisch, G.W. Trucks, H.B. Schlegel, G.E. Scuseria, M.A. Robb, J.R. Cheeseman, G. Scalmani, V. Barone, G.A. Petersson, H. Nakatsuji, X. Li, M. Caricato, A.V. Marenich, J. Bloino, B.G. Janesko, R. Gomperts, B. Mennucci, H.P. Hratchian, J.V. Ortiz, A.F. Izmaylov, J.L. Sonnenberg, Williams, F. Ding, F. Lipparini, F. Egidi, J. Goings, B. Peng, A. Petrone, T. Henderson, D. Ranasinghe, V.G. Zakrzewski, J. Gao, N. Rega, G. Zheng, W. Liang, M. Hada, M. Ehara, K. Toyota, R. Fukuda, J. Hasegawa, M. Ishida, T. Nakajima, Y. Honda, O. Kitao, H. Nakai, T. Vreven, K. Throssell, J.A. Montgomery Jr., J.E. Peralta, F. Ogliaro, M.J. Bearpark, J.J. Heyd, E.N. Brothers, K.N. Kudin, V.N. Staroverov, T.A. Keith, R. Kobayashi, J. Normand, K. Raghavachari, A.P. Rendell, J.C. Burant, S.S. Iyengar, J. Tomasi, M. Cossi, J.M. Millam, M. Klene, C. Adamo, R. Cammi, J.W. Ochterski, R.L. Martin, K. Morokuma, O. Farkas, J.B. Foresman, D.J. Fox, Gaussian 09, Revision E.01, Wallingford, CT, 2009.

[44] H.-J. Werner, P.J. Knowles, G. Knizia, F.R. Manby, M. Schütz, P. Celani, T. Korona, R. Lindh, A. Mitrushenkov, G. Rauhut, K.R. Shamasundar, T.B. Adler, R.D. Amos, A. Bernhardsson, A. Berning, D.L. Cooper, M.J.O. Deegan, A.J. Dobbyn, F. Eckert, E. Goll, C. Hampel, A. Hesselmann, G. Hetzer, T. Hrenar, G. Jansen, C. Köppl, Y. Liu, A.W. Lloyd, R.A. Mata, A.J. May, S.J. McNicholas, W. Meyer, M.E. Mura, A. Nicklass, D.P. O'Neill, P. Palmieri, K. Pflüger, R. Pitzer, M. Reiher, T. Shiozaki, H. Stoll, A.J. Stone, R. Tarroni, T. Thorsteinsson, M. Wang, A. Wolf, MOLPRO, Version 2010.1, a Package of Ab Initio Programs.

[45] S. Li, Threshold Photoionization and ZEKE Photoelectron Spectroscopy of Metal Complexes, University of Kentucky, 2004.

[46] E.V. Doktorov, I.A. Malkin, V.I. Man'ko, FC calculations in FCF program 1 (dynamical symmetry of vibronic transitions in polyatomic molecules and the Frank-Condon principle), J. Mol. Spectrosc. 64 (2) (1977) 302–326.

[47] F. Duschinsky, The Importance of the electron spectrum in multiatomic molecules. Concerning the Franck-Condon principle, Acta Physicochim 7 (4) (1937) 551–566.

[48] F.M. Fraser, E.J. Prosen, Heats of combustion and isomerization of six pentadienes and spiropentane, J. Res. Natl. Bur. Stand. (U.S.) 54 (1955) 143–148. Research Paper No. 2575.

[49] D.D. Wagman, J.E. Kilpatrick, K.S. Pitzer, F.D. Rossini, Heats, equilibrium constants, and free energies of formation of the acetylene hydrocarbons through the pentynes, to 1500 K. J. Res. Natl. Bur. Stand. (U.S.) 35 (6) (1945) 467–496.